Holme, R. T., Whaler, K. A. (2001): Steady core flow in an azimuthally drifting reference frame. - Geophysical Journal International, 145, 2, pp. 560—569.

DOI: https://doi.org/10.1046/j.1365-246x.2001.01436.x

Geophys. J. Int. (2001) **145,** 560–569

Steady core flow in an azimuthally drifting reference frame

R. Holme[1] and K. A. Whaler[2]

[1] *GeoForschungsZentrum Potsdam, Telegrafenberg,* D-14473 *Potsdam, Germany. E-mail: holme@gfz-potsdam.de*
[2] *Department of Geology and Geophysics, University of Edinburgh, Grant Institute, West Mains Road, Edinburgh,* EH9 3JW, *UK*

Accepted 2001 January 26. Received 2000 December 6; in original form 1999 August 18

SUMMARY

Flows at the top of the Earth's core generating the observed geomagnetic secular variation (SV) can be deduced in the frozen-flux approximation with various non-uniqueness-reducing assumptions such as tangential geostrophy and steadiness. Steady flows are attractive because they require only a small number of parameters to explain the gross features of the SV. However, they are unable to reproduce the fine detail contained in the SV, and cannot be used to explain observed decadal changes in the length of day. Here we find flows steady in a local reference frame within the core, but the frame is allowed to rotate relative to the mantle. Previous investigations have studied steady drift with respect to the mantle, introducing just a single extra parameter into the calculation; here we also allow the drift to vary with time. We then minimize a linear combination of the fit to time-varying coefficients expressing the SV, a measure of the complexity of the flow and the drift acceleration. The resulting non-linear inverse problem is solved in a two-stage iterative process—for a given drift, we solve for the best-fitting steady flow, and then adjust the drift to improve the fit. We seek solutions for the intervals 1900–1980 and 1840–1990; over both epochs, allowing the reference frame of a steady flow to drift gives a strikingly improved fit. For flows with a relatively high misfit, the frame drift is westwards at a rate similar to the observed 'westward drift' rate of the geomagnetic field at the Earth's surface (approximately 0.2° yr^{-1}). Requiring a tighter fit, and hence a more complex flow, gives rise to two solutions, one with a westward frame drift with respect to the mantle, the other eastward, and the relative drift rates gradually increase to a maximum of 0.9° yr^{-1} as the misfit decreases. Flows in the mantle reference frame are similar to those deduced previously by any of the non-uniqueness-reducing assumptions. However, in the drifting frame, the flows are almost completely dominated by the drift between the two reference frames. Although the time dependence of the drift is weak and results in only a small additional misfit reduction over a uniform drift, by assuming that the variation in drift reflects variation in solid body rotation of the whole core, it can explain decadal length-of-day changes almost as well as, and prior to 1900 perhaps better than, fully time-dependent tangentially geostrophic flows with vastly more free parameters. We examine the significance of these models in terms of large-scale wave motion in the core.

Key words: core–mantle boundary, Earth's rotation, flow imaging, geomagnetism, wave motion.

1 INTRODUCTION

The temporal evolution (secular variation) of the geomagnetic field provides a powerful tool for probing the physics of the deep Earth, in particular conditions at the top of the core. Following Roberts & Scott (1965), one particular application has been to use the secular variation to estimate the flow at the surface of the core. If changes in the magnetic field are due principally to fluid advection of the field, rather than its diffusion (the so-called 'frozen-flux' approximation), then the radial component of the magnetic induction equation provides a constraint on core surface flow. Roberts & Scott (1965) recognized that the determination of the flow is formally non-unique; this non-uniqueness was quantified by Backus (1968). To understand this intuitively, we have one equation at every point on the core–mantle boundary (CMB) from which to

determine two unknowns, the two orthogonal components of surface velocity. Subsequent work has focused on trying to reduce or remove this non-uniqueness by making various *a priori* assumptions about the nature of the flow. The most common such assumptions have been that the flow is purely toroidal (the dynamics at the top of the core is assumed dominated by stable stratification; Whaler 1980; Bloxham 1990), tangentially geostrophic (the Lorentz force is small at the CMB, so the horizontal force balance is dominantly between the pressure gradient and the Coriolis force; Hills 1979; Le Mouël *et al.* 1985; Backus & Le Mouël 1986) or steady in time (Gubbins 1982; Voorhies & Backus 1985). Modelling of core–surface flow is reviewed in detail by Bloxham & Jackson (1991) and Whaler & Davis (1997).

The steady flow assumption is particularly attractive from a reductionist point of view, as it requires very few parameters to explain almost all of the observed secular variation. Variance reduction of over 90 per cent is standard (e.g. Bloxham 1992), and it can exceed 98 per cent (Voorhies 1986). However, this assumption has several drawbacks. First, although a steady flow can fit the gross features of the observed secular variation, it is unable to fit the fine-scale time variation, in particular the well-defined time variation shown by annual means from magnetic observatories, and is unable to reproduce sharp changes in secular variation, the so-called 'geomagnetic jerks' (Courtillot *et al.* 1978; Malin *et al.* 1983). Second, it is unclear what physical significance to assign to the flow model obtained; Gubbins & Kelly (1996) have argued that a steady flow will naturally lead to a balance between advection and diffusion, so the neglect of diffusion via the frozen-flux approximation is not valid. Third, a steady flow cannot be used to estimate changes in core angular momentum and its correlation with observed decadal variation in length of day (ΔLOD).

The rate of rotation of the Earth varies on all observable timescales. One of the largest signals is a ΔLOD of a few milliseconds on decadal timescales. For many years, this signal has been attributed to angular momentum exchange between the fluid core and solid mantle, at least in part because no other observed motion (for example, oceanic or atmospheric) is of sufficient magnitude on such timescales. However, this supposition was put on a much firmer footing by Jault *et al.* (1988), who argued that on decadal timescales the core would respond to changes in angular momentum by motions uniform on cylinders coaxial with the Earth's axis of rotation, so-called torsional oscillations (Braginsky 1970). If this is true, then changes in surface flow reflect motions deep within the core, allowing the calculation of changes in angular momentum of the whole core. Such calculations are in remarkable agreement with the change in angular momentum required to explain the observed variations in the rotation of the mantle, at least for this century (Jault & Le Mouël 1989; Jackson *et al.* 1993; Jackson 1997). This agreement is important, as it is the only independent evidence that, despite all the required assumptions in the flow derivation (neglect of diffusion, large-scale flow, simplistic assumptions about flow dynamics), the flow models we obtain are meaningful. Clearly, a steady flow cannot be used for such a calculation, as it would imply constant angular momentum.

A simple generalization of the steady flow assumption that might overcome some of these problems is the consideration of steady flow in an azimuthally drifting frame, an approach first suggested by Voorhies & Backus (1985). In this approach, the flow is considered to be steady in a frame fixed in the core, but the core frame is allowed to rotate with respect to the mantle about the Earth's rotation axis. The physical basis for this assumption is a separation of timescales related to the core. Torsional oscillations aside, the dynamics of the core are thought to vary on a long timescale—for example, one of the most rapid timescales associated with its behaviour, that of MAC (magnetic–Archimedean–Coriolis) waves, is of the order of hundreds of years (Gubbins & Roberts 1987). This slow evolution also provides a dynamical justification for the steady flow assumption (Davis & Whaler 1996a). However, decadal ΔLOD are by definition on a shorter timescale. Imagine that the concentric cylinders supporting the torsional oscillations are welded together, perhaps by means of a strong magnetic field in the cylindrically radial direction, so that the torsional oscillations are approximated by a solid body rotation of the core. Changes in this rotation can then appear in the model as changes in the drift rate.

Davis & Whaler (1996a) examined the effect of a steady drift over successive short (10 yr) epochs; here we extend this work to consider longer epochs, first 1900–1980 and then 1840–1990. We first consider a steady drift rate; this adds only one additional free parameter over considering a steady flow, but like the steady flow cannot be used to explain ΔLOD. We then generalize to a time-dependent drift, and consider the implications for the angular momentum budget. Finally, we consider in some detail the possible geophysical implications of our results.

2 THEORY

Models of flow at the core surface $\mathbf{u}$ are generally determined using the radial component of the frozen-flux induction equation,

$$\dot{B}_r + \nabla_H \cdot (B_r \mathbf{u}) = 0\,, \tag{1}$$

where B_r is the radial component of the magnetic field at the CMB, the dot denotes a time derivative, and $\nabla_H \cdot$ is the horizontal divergence operator. To reduce non-uniqueness, it is usual to make additional assumptions about the nature of the flow. Here, we assume that the flow is steady in a frame of reference that can 'drift' (rotate) azimuthally with respect to the mantle. In geocentric spherical coordinates (r, θ, ϕ), and denoting quantities in the drifting frame with primes, to transform from the stationary (mantle) frame to the drifting (core) frame, we take

$$\phi' + \psi = \phi\,, \tag{2}$$

where ψ is the accumulated drift angle (positive eastwards). The flow in the mantle frame is then calculated from the steady flow in the drifting frame $\mathbf{u}'$ by

$$\mathbf{u}(\theta, \phi, t) = \mathbf{u}'(\theta, \phi - \psi(t)) + r_c \dot{\psi} \cos\theta \hat{\boldsymbol{\phi}}\,, \tag{3}$$

where r_c the core radius and $\hat{\boldsymbol{\phi}}$ the unit vector in the azimuthal direction. In principle it would be possible to solve for $\mathbf{u}$ directly. However, it is more straightforward to work in the drifting

frame and solve

$$\dot{B}_r{}' + \nabla_H.(B_r{}'\mathbf{u}') = 0\,. \tag{4}$$

To determine the radial field and secular variation in the drifting frame, we adopt the usual magnetic scalar potential

$$\Phi = r_e \sum_{l=1}^{\infty} \left(\frac{r_e}{r}\right)^{l+1} \sum_{m=0}^{l} P_l^m(\cos\theta)\left[g_l^m \cos(m\phi) + h_l^m \sin(m\phi)\right], \tag{5}$$

where the magnetic field $\mathbf{B} = -\nabla\Phi$. $P_l^m(\cos\theta)$ are Schmidt-normalized associated Legendre polynomials of degree l and order m, $r_e = 6371.2$ km is the mean radius of the Earth and $\{g_l^m, h_l^m\}$ is the set of Gauss coefficients that define the field. From Galilean invariance, $\mathbf{B}$ must be the same whether calculated in the stationary or drifting frame. Using spherical harmonic orthogonality we have

$$\begin{aligned} &g_l^m \cos m(\phi' + \psi) + h_l^m \sin m(\phi' + \psi) \\ &\quad = g_l^{m\prime} \cos(m\phi') + h_l^{m\prime} \sin(m\phi')\,, \end{aligned} \tag{6}$$

so the Gauss coefficients in the drifting frame are

$$\begin{aligned} g_l^{m\prime} &= g_l^m \cos m\psi + h_l^m \sin m\psi\,, \\ h_l^{m\prime} &= h_l^m \cos m\psi - g_l^m \sin m\psi\,. \end{aligned} \tag{7}$$

The secular variation coefficients in the drifting frame are then

$$\begin{aligned} \dot{g}_l^{m\prime} &= \dot{g}_l^m \cos m\psi + \dot{h}_l^m \sin m\psi + m\dot{\psi} h_l^{m\prime}, \\ \dot{h}_l^{m\prime} &= \dot{h}_l^m \cos m\psi - \dot{g}_l^m \sin m\psi - m\dot{\psi} g_l^{m\prime}, \end{aligned} \tag{8}$$

that is, the usual coefficients rotated into the drifting frame plus a contribution from the relative velocity between the two frames.

3 IMPLEMENTATION

We seek a drift rate for the steady flow with respect to the mantle that allows us to minimize the following objective function:

$$\mathcal{O} = \int_{t_0}^{t_1} \left[\int_{r_c} \left(\dot{B}_r - \dot{B}_r{}^0\right)^2 dS + \lambda_d (\ddot{\psi})^2 \right] dt + \lambda_v N\,. \tag{9}$$

The three components of this function are the misfit to $\dot{B}_r{}^0$, the secular variation at the Earth's surface, the mean square angular acceleration of the drifting frame with respect to the mantle, and a quadratic norm N of the velocity coefficients in the drifting frame [we adopt the commonly used norm

$$N = \oint_{CMB} \left[(\nabla_H^2 u_\theta)^2 + (\nabla_H^2 u_\phi)^2 \right] dS \tag{10}$$

of Bloxham (1988)], which regularizes the flow inversion. The inversion is controlled by two damping parameters: λ_v, which controls the complexity of the steady flow in the drifting frame, and λ_d, which restricts the degree of time dependence of the drift. The misfit to the secular variation is most easily calculated in the drifting frame: because the transformation from steady to drifting frame is the same for the model secular variation coefficients and those predicted by the flow, the misfit is invariant to the rotation of the reference frame. The secular variation integral is approximated by discrete samples calculated at 1 yr intervals.

For a given drift, the flow is parametrized as is usual (e.g. Bloxham & Jackson 1991) by decomposing it into its poloidal and toroidal parts, writing

$$\mathbf{u} = \nabla_H(rS) + \nabla_H \wedge (T\mathbf{r})\,. \tag{11}$$

The poloidal and toroidal scalars are then expanded in Schmidt-normalized real spherical harmonics, writing

$$\begin{aligned} S &= \sum_{l,m} \left(s_l^{mc} \cos(m\phi) + s_l^{ms} \sin(m\phi)\right) P_l^m(\cos\theta)\,, \\ T &= \sum_{l,m} \left(t_l^{mc} \cos(m\phi) + t_l^{ms} \sin(m\phi)\right) P_l^m(\cos\theta)\,. \end{aligned} \tag{12}$$

For known drift, eq. (4) can then be reduced to a set of linear equations for the flow coefficients $\{t_l^m, s_l^m\}$ (Whaler 1986). We calculate the main geomagnetic field and secular variation at each epoch using the ufm time-dependent field model of Bloxham & Jackson (1992). Using this model also allowed us to fit the secular variation coefficients weighted by their uncertainties derived from diagonal elements of the covariance matrix, instead of minimizing secular variation misfit as in eq. (9); we find that the different weighting has little effect on our results, in agreement with the conclusions of Jackson *et al.* (1993). The harmonic expansions for magnetic field, secular variation and flow are all truncated at degree $l = 14$.

We parametrize the accumulated drift angle between drifting and mantle reference frames ψ [as opposed to the drift rate as in the previous studies of Davis & Whaler (1996a,b)] as a function of time on the basis of cubic B-splines (de Boor 1978) with a 2.5 yr knot spacing, allowing easy calculation of the instantaneous drift rate $\dot{\psi}$ and acceleration $\ddot{\psi}$. The B-spline coefficients for the drift angle are allowed to vary, and for each choice of coefficients the best-fitting flow is obtained by a standard regularized least-squares fit to the secular variation coefficients. The optimum set of spline coefficients is then obtained using Powell's method (e.g. Press *et al.* 1986). We choose this method because it does not require the calculation of the derivative of the objective function with respect to the drift angle coefficients, the determination of which would be extremely complicated. Whilst the predicted secular variation in the drifting frame, $\dot{B}_r{}'$, depends linearly on the flow, its transformation into the mantle frame, $\dot{B}_r$, depends non-linearly on both the drift angle and drift rate. In effect, we split our inversion into two parts, using a search method for the non-linear terms, and solving the linear flow problem at each stage of the non-linear search.

At this point, it is worth emphasizing the difference between the drift rate parameter that we have described and the solid body rotation term in the flow expansion, t_1^0 in eq. (12). A non-zero drift contributes directly to the secular variation in the same way as the uniform toroidal flow (through the final right-hand-side terms in eqs 8). If the flow $\mathbf{u}$ was zonally symmetric (only $m = 0$ terms non-zero in eq. 12) then the two would be equivalent. However, a non-zero drift also rotates the non-zonal part of the flow with respect to the mantle, whereas changing the t_1^0 component of the flow does not alter the other flow components. Furthermore, only the frame of reference of the flow generating the secular variation rotates with respect to the mantle, not the magnetic field or its secular variation. This rotation could be considered as a very simple wave motion of flow structure, angular velocity $\dot{\psi}$. We return to this point in more detail in Section 7.

4 RESULTS

We first investigate the broad-scale effect of varying drift rate. We define the B-spline coefficients to give a predefined, uniform drift rate (so that $\ddot{\psi}=0$), and calculate the optimum steady flow between 1900 and 1980 for a variety of damping parameters λ_v. In Fig. 1 we plot the objective function $\mathcal{O}$ (eq. 9) as a function of drift rate from solutions that are clearly overdamped (they do not provide an adequate fit to the model of secular variation) to solutions that are clearly underdamped (the flow is unreasonably strong, and there is too much power in high-degree flow components for the flow to be considered properly converged). Heavily damped flows are very weak, and the optimum drift rate is slightly below $0.2^\circ\,\mathrm{yr}^{-1}$ westwards, close to the customary estimate of westward drift at the Earth's surface. In this solution, the drift adopts the role of the t_1^0 flow component, allowing the flow norm to be minimized. However, as the damping parameter is reduced, allowing a stronger flow and hence a closer fit to the secular variation model, the magnitude of the drift increases. Perhaps more interestingly, a second solution appears with positive (eastward) drift, although this solution is slightly less favourable in terms of minimizing the objective function. Davis & Whaler (1996a) also found an eastward solution for one of their 10 yr epochs.

We examine solutions for three damping parameters in more detail, corresponding to the second, third and fourth lines from the bottom of Fig. 1. For each of these parameters (which we characterize respectively 'weak', 'medium' and 'strong' damping) we first optimize for a uniform drift rate $\dot{\psi}=$constant, seeking local minima in the objective function with both eastward and westward steady drift. Then, starting from these uniform solutions, we obtain solutions with time-dependent drift. The solution is not sensitive to fine details of the starting model; with a different choice for initial uniform drift or an arbitrary initial time dependence, the inversion still converges on one of the two solutions (positive or negative drift)—it just takes much longer! The objective function turns out to be insensitive to the temporal damping parameter λ_d; we adjust this merely to prevent variations in the drift more rapid than our 'data' sampling rate (in general every 2.5 yr). The redundancy of this parameter arises because of the smooth properties of the secular variation model ufm that we are fitting.

In Fig. 2 we plot the rms misfit to ufm secular variation against the solution norm for the three chosen damping parameters λ_v. For each damping parameter, we plot diagnostics for a steady flow (included in Fig. 1 as the case for drift rate $=0.0^\circ\,\mathrm{yr}^{-1}$) and for optimized drifts, both steady and time-dependent, and both westward and eastward. Clearly, allowing for a drifting frame enables a striking improvement to the fit to the secular variation model for little increase (and for weak damping a small *decrease*) in the complexity of the steady flow (as measured in the drifting frame). To think of this in another way, compare the weakly damped steady flow and medium damped drifting flows. For only one additional free parameter (in the case of steady drift), the model of secular variation is fitted just as well with a flow with the norm reduced by an order of magnitude. However, there is surprisingly little additional improvement in fit obtained by allowing a time-dependent, rather than uniform, drift.

In Fig. 3 we compare the fit to the secular variation model of the predictions due to a steady flow, a steady drift and a time-dependent drift. For illustration we plot the results from the eastward-drifting, weakly damped solutions. As would be expected from Fig. 2, the drifting flow produces a great improvement in the fit to the coefficients, but the time-dependent drift produces little further improvement. The steady flow allows recovery of the mean secular variation and a slowly varying trend, but allowing the frame to drift achieves a much better representation of the decadal period time variation of the secular variation. In particular, note the fit to the so-called '60-year oscillation' in the $\dot{g}_1^0$ and $\dot{g}_3^0$ coefficients from a process that is physically steady (a steady flow in a uniformly drifting frame). However, the drifting flow does not easily model more rapid fluctuations in secular variation, which can be fitted by a fully time-dependent flow (see e.g. Jackson 1997). This may be an advantage; variations in secular variation in ufm at periods close to 11 yr suggest a possible relationship to the solar cycle

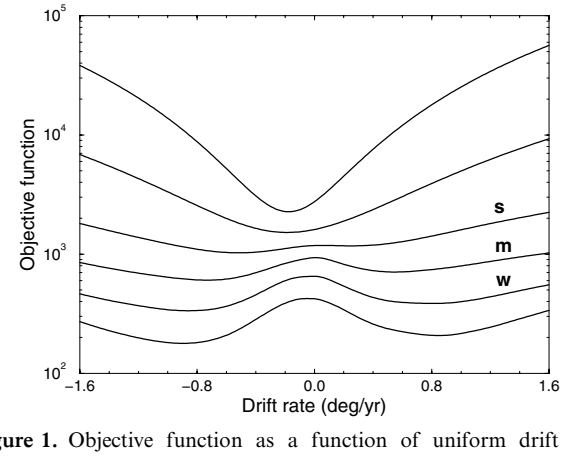

Figure 1. Objective function as a function of uniform drift rate (eastward positive) for a variety of damping parameters. The value of the damping parameter λ_v is decreased by a factor of 10 between each curve, from 0.2 (top curve) to 2.0×10^{-6} (bottom curve). We subsequently focus on three values of damping parameter, labelled w (weakly damped: $\lambda_v=2.0\times10^{-5}$), m (medium damping: $\lambda_v=2.0\times10^{-4}$) and s (strongly damped: $\lambda_v=2.0\times10^{-3}$).

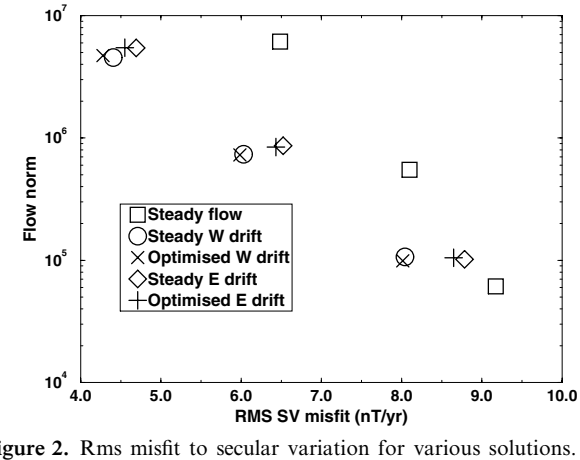

Figure 2. Rms misfit to secular variation for various solutions. For each damping parameter, the solution norm N does not change significantly with the introduction of drift. Thus the five points with highest norm are for $\lambda_v=2\times10^{-5}$ (weak damping), the five middle points are for $\lambda_v=2\times10^{-4}$ (medium damping) and the five lowest points are for $\lambda_v=2\times10^{-3}$ (strong damping).

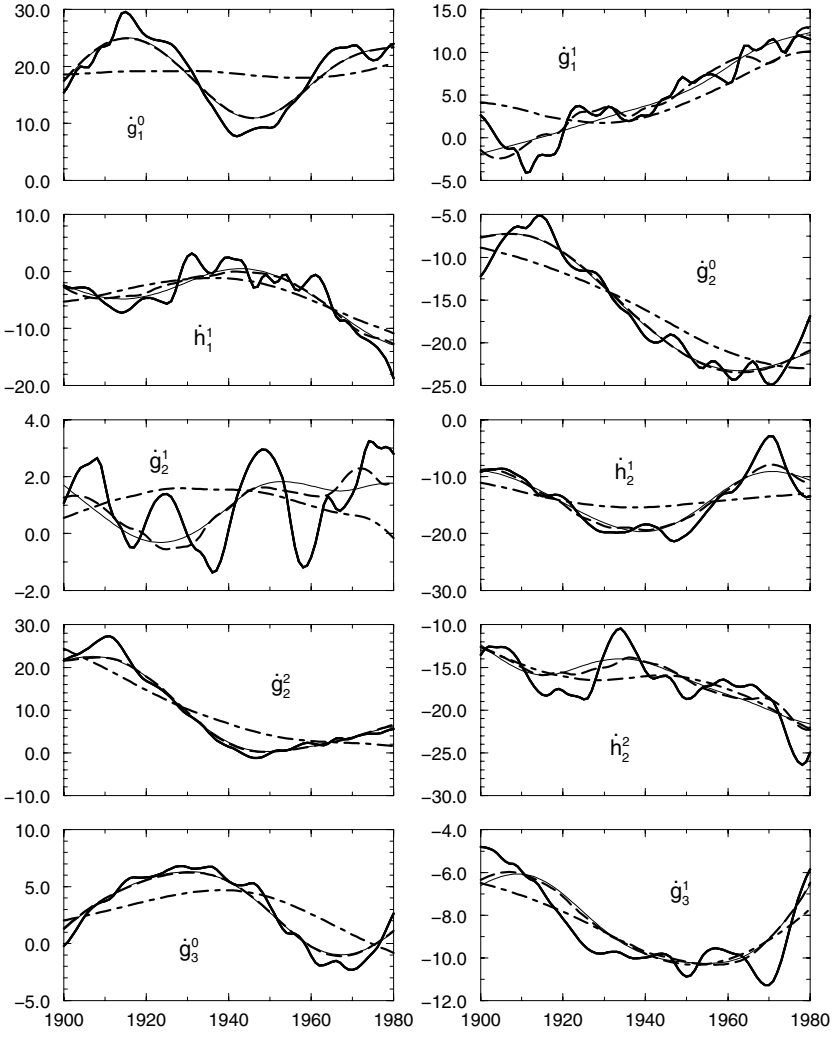

Figure 3. The first eight ufm secular variation model coefficients (thick solid line) compared with predictions due to steady flow (dot-dashed line), steady drift (thin solid line) and time-varying drift (dashed line). Note in particular the improved fit allowed by the drifting frame solutions to the '60-year oscillation' in the $\dot{g}_1^0$ and $\dot{g}_3^0$ coefficients. Weakly damped, eastward-drifting solutions chosen. All vertical axes in nT yr^{-1}, horizontal axes in yr.

and contamination of the model with fields originating external to the Earth. However, as a consequence, the drifting flows do not explain geomagnetic jerks (for example, the sharp change shown by many secular variation coefficients of ufm around 1970, particularly $\dot{h}_2^1$ and $\dot{g}_3^1$).

In Table 1 we list the apparent flow strength in the mantle frame for the various solutions shown in Fig. 1. The addition of drift generally results in weaker apparent flows. This is a general feature of allowing time dependence in a flow model—the increased degrees of freedom for the flow mean that it requires less small-scale structure to explain the secular variation, and so a weaker flow is allowed. The westward-drifting steady flows produce a slightly lower apparent flow strength than the eastward-drifting flows.

Table 1. Rms flow speeds in a mantle reference frame for solutions plotted in Fig. 2. All values in km yr^{-1}.

Damping	No drift	W drift		E drift	
		Steady	Optimized	Steady	Optimized
Weak	20.1	12.9	13.2	14.5	15.1
Medium	14.0	9.8	9.9	11.1	11.2
Strong	10.7	8.6	8.8	10.8	10.9

In Fig. 4 we plot the drifting flow solutions for weak damping for both westward (left column) and eastward (right column) drift. The top three plots are snapshots in time in the mantle frame; the fourth plot is of the flow in the drifting frame in the core. The drift angle ψ is defined to be zero in 1900, so the two frames are coincident at that time. The drifting flow reproduces some features seen in time-dependent flows for this period. We see strong westward flow near the equator along a band straddling the equator in the hemisphere centred on the Greenwich meridian, weaker or even eastward flow beneath the Pacific hemisphere, and a large anticlockwise gyre in the southern hemisphere near Africa, especially in the westward-drifting flow, although its position under the southern Indian Ocean is offset slightly eastwards from previous work. The structure of the steady flow results in a change in apparent flow direction beneath the US Atlantic coast around the middle of the century, which is also a feature of some previous flow models (e.g. Bloxham 1989). That our flows look similar to

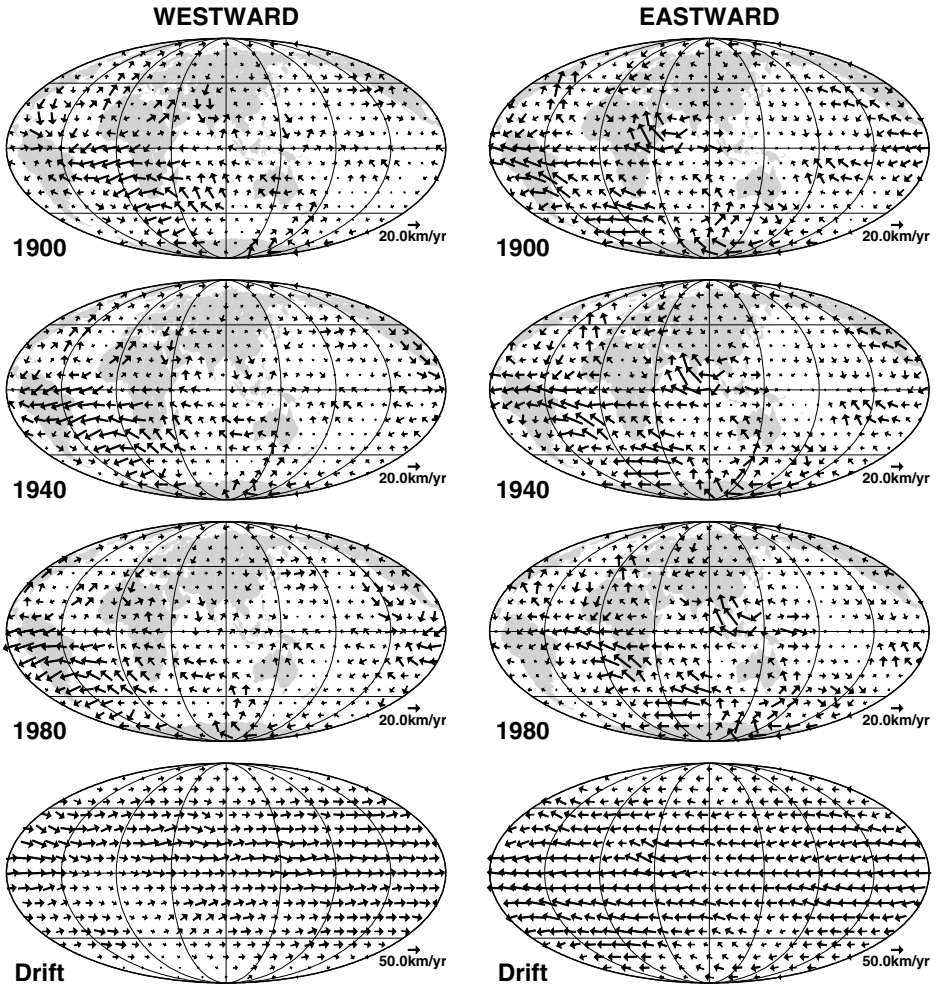

Figure 4. Maps of drifting flow for the 'weak damping' solutions. The continents are projected onto the core's surface to provide a reference frame. The left-hand column plots the solution for westward drift ($\dot{\psi} < 0$), the right-hand column for eastward drift ($\dot{\psi} > 0$). In each case, the top three maps are snapshots of the apparent flow observed in the mantle reference frame at three different times, and the fourth map shows the steady flow in the drifting reference frame. The two reference frames are defined to be coincident in 1900. Note the change in scale for the bottom pair of plots. The map projection is Mollweide equal area. The plots are produced with GMT (Wessel & Smith 1991).

previously determined flows is not surprising; we are fitting the same data within a similar theoretical framework. To achieve such 'normal'-looking flows, however, the flow in the drifting frame is anything but normal. Note in particular the different scale used for the flow arrows for the drifting-frame flows, which are dominated by a large backflow in the opposite sense to the drift. The drifting frame is effective because it can move non-zonal features in the steady flow around in time, but this would also result in an unobserved large bulk rotation in the magnetic field. To counter this, the associated steady flow must include a large opposing uniform zonal (t_1^0) flow. Mathematically, this term is required to balance the contribution from the final right-hand-side terms in eqs (8).

The requirement for a large zonal flow to counter the drift also explains much of the dependence of the optimal drift rates on the damping parameter λ_v, including the preference for westward rather than eastward drift. We plot optimal steady drift rates (the positions of the local minima in Fig. 1) as a function of λ_v, together with values for the particular solutions from Fig. 2, in Fig. 5. As previously noted, when the solution is

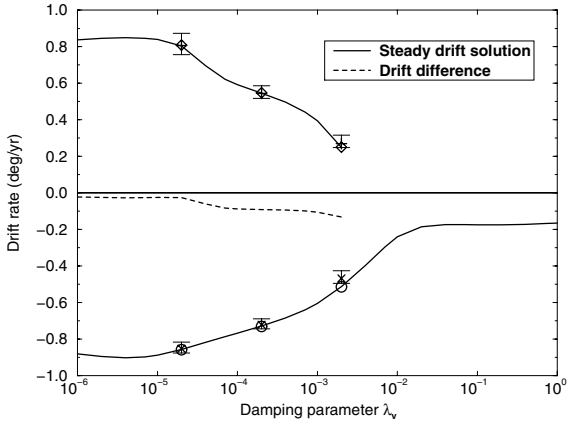

Figure 5. Optimal steady drift rate as a function of damping parameter. Where two solutions exist, their difference is plotted as the dashed line. The various symbols correspond to the solutions shown in Fig. 2, with the 'error bars' showing the range of drift rates between 1900 and 1980 for the optimized solutions.

strongly overdamped (right-hand edge of the figure), only one solution is obtained, with drift rate just less than -0.2° yr^{-1}, to allow the flow velocity to be minimized. For weaker damping, two solutions are present, initially equidistant from the overdamped solution (demonstrated by the dashed line giving the mean of the two drift rates). The net t_1^0 flow in the mantle frame is the same in both cases, a few kilometres per year westwards at the equator, and to achieve this a larger backflow is required for the eastward-drifting solution than for the westward-drifting solution, leading to a larger contribution to the objective function (9), and so a preference for the westward-drifting solution. As damping is further reduced, the drift rate magnitudes increase, the influence of the flow norm diminishes and the westward- and eastward-drifting solutions are approximately symmetric about 0.0° yr^{-1}, indicating that the secular variation model (as distinct from the objective function) shows no preference between eastward and westward drift. Note also from Fig. 2 that the diagnostics of the two solutions converge for weaker damping. We also plot in Fig. 5 'error bars' for the optimized solutions, showing the range of variation of the drift about its mean value. That this range is small—of the order of $\pm 0.05^\circ$ yr^{-1} variations about the mean drift rate—explains in part why allowing time-dependent drift produces little improvement in the fit to the secular variation above that obtained with a steady drift.

5 THE CORE–MANTLE ANGULAR MOMENTUM BUDGET

From the perspective of improving the fit to the secular variation model, it would be difficult to justify a time-dependent drift. For the addition of many more degrees of freedom in the solution, we obtain a negligible improvement in the fit over the single extra parameter, uniform drift solution. Nevertheless, we examine further the implications of time-dependent drift, assuming that the variation in our surface drift rate is a reflection of a solid-body rotation of the whole core, and compare the time variation with that required to explain the observed ΔLOD [taken from McCarthy & Babcock (1986), with an estimate of the tidal signal subtracted (Jackson *et al.* 1993)]. In Fig. 6 we present three plots that compare the predicted length-of-day variation for various flows. In (a) we present the predictions for the three westward-drifting flows, in (b) the predictions for the three eastward-drifting flows, and finally, for comparison, in (c) the earlier results of Jackson *et al.* (1993) for a sequence of single epoch, tangentially geostrophic flows, based on the theory of torsional oscillations of Jault *et al.* (1988). In this theory, the predicted variation in length of day is given by

$$\Delta\mathrm{LOD} = 1.138\left(\Delta t_1^0 + \frac{12}{7}\,\Delta t_3^0\right), \tag{13}$$

where ΔLOD is in milliseconds and the Schmidt-normalized flow coefficients (eq. 12) are in kilometres per year (Jackson *et al.* 1993). Note that only two of the toroidal flow components, t_1^0 and t_3^0, contribute to the angular momentum budget. The equivalent expression for a drifting reference frame is

$$\Delta\mathrm{LOD} = 69.2\Delta\dot{\psi}\ , \tag{14}$$

where $\dot{\psi}$ is measured in degrees per year. In both cases, only changes in LOD are resolved; the vertical offset for each curve can be varied freely, and has been chosen to facilitate clear representation of the results.

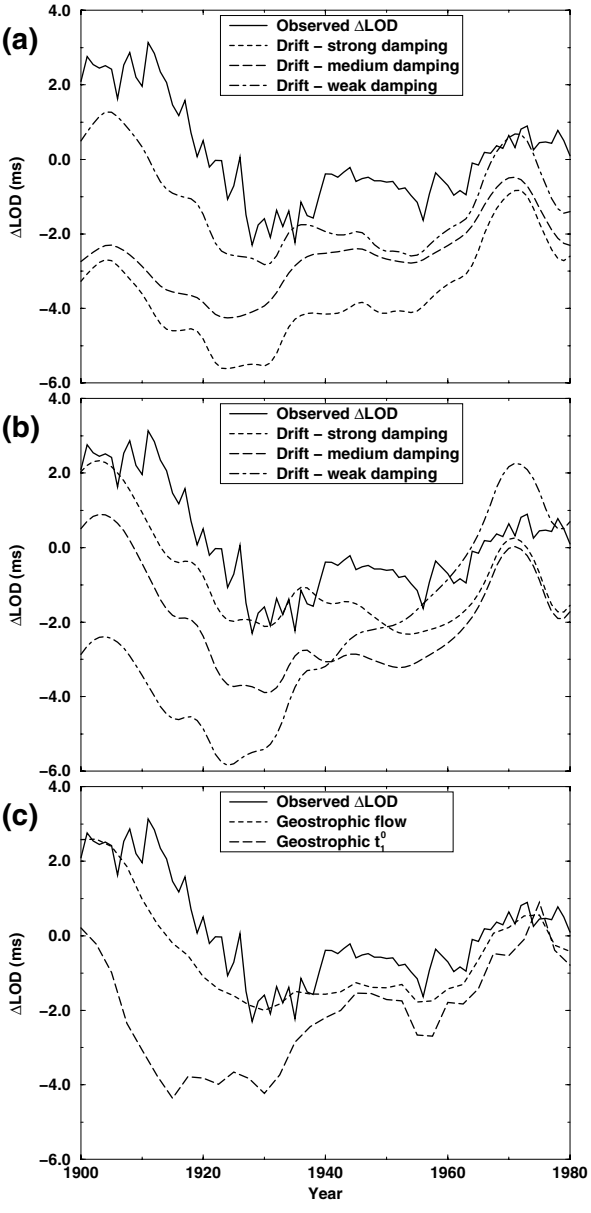

Figure 6. LOD correlation with that predicted from various flows. (a) Calculated from core drift rate for westward-drifting solutions. (b) Calculated from core drift rate for eastward-drifting solutions. (c) Calculated from tangentially geostrophic flows of Jackson *et al.* (1993), including that predicted from the uniform zonal flow component t_1^0 alone. For all three cases, the vertical offset is arbitrary; on each plot the curves are separated for clarity.

The LOD signal is robust enough to emerge even with our simplified model of the torsional dynamics, and despite the minimal contribution to the fit to the secular variation from adding time dependence to the drift (in Fig. 3 the difference between the thin solid line and the dashed line). The variability is well described in each case and is robust to drift rate; in particular a peak in the curves at 1910 and a flat trough around 1925. The sharp peak at 1970 is not a feature of the ΔLOD curve, and may be related to the poor fit of our flow model to the secular variation around the time of the 1970 geomagnetic jerk. The main mismatch is that drifting flows produce a steady trend not present in the data. The match of the single-epoch tangentially geostrophic flows of Jackson *et al.* (1993) is slightly

closer, although that fit requires far more free parameters than our drifting flow models. Furthermore, it is noticeable that some of the drifting solutions provide a closer match than the t_1^0 curve of Jackson *et al.* (1993) (the part of the flow corresponding to solid body rotation), again demonstrating the difference between the drifting frame and a simple zonal t_1^0 flow.

Another way to investigate the presence of an Earth rotation signal in the drifting flows is to invert for a mean drift rate with the time dependence $\Delta\dot{\psi}$ defined proportional to the smoothed ΔLOD. Like the uniform drift rate calculations, this adds only one free parameter to the steady flow solution. For the weakly damped solution with westward drift, and for all three solutions with eastward drift, such a model provides a better solution (smaller objective function and closer fit to the secular variation coefficients) than a uniform drift, providing further evidence that a ΔLOD signal is present in the data.

6 THE PERIOD 1840–1990

We have concentrated thus far on the period 1900–1980. Here we extend our analysis to 1840–1990. The field model is less reliable prior to 1900, as the data from this period are generally fewer, of a lower quality and with a less uniform distribution (see Bloxham *et al.* 1989, for a discussion of the data used to constrain ufm). Visible edge effects in model behaviour at 1840 and 1990 suggest that the values for the secular variation and in particular its time derivative, the secular acceleration, may be less reliable at these times, which could lead to systematic errors in the flows determined at these epochs. Furthermore, the physical motivation for the steady flow is that the interval considered is short compared with the dynamical timescales within the core; for 150 yr it is no longer so clear that this temporal separation applies. Nevertheless, it is of interest to consider the behaviour of the drifting flow solution over this longer interval.

In Fig. 7 we plot the objective function for uniform drift as a function of drift rate. Comparing with Fig. 1 for the shorter period, the value for the objective function is slightly higher in each case, as it is more difficult for a steady flow to fit the time-dependent secular variation over a longer period. However, allowing for a drifting reference frame still significantly improves the solution obtained. In comparison with the shorter time interval, the limiting value for the drift at low damping is slightly reduced, and where both westward- and eastward-drifting solutions are present, the preferred solution (minimum objective function) is now eastward drifting. This is an interesting result given our earlier comments concerning the influence of damping and the norm on the preferred solution for the interval 1900–1980. The choice between the two solutions depends on the particular time and length of epoch analysed, and it seems safest to observe that the evidence is insufficiently strong to prefer one drift direction over the other. This may explain the surprising result of Davis & Whaler (1996a) of a switch from a reasonably fast westward- to an equally fast eastward-drifting solution between two successive 10 yr epochs.

In Fig. 8 we consider the predicted ΔLOD for one of these eastward-drifting flows (the second curve from the bottom of Fig. 7, marked w, corresponding to the 'weakly damped' solution described earlier). For comparison we also present the results of Jackson *et al.* (1993) for their sequence of tangentially geostrophic flows. While the comparison with the observed variations in Earth rotation is not as good post-1900, it is at least as good, and arguably better, prior to 1900. The drifting solution is also a considerably better fit to the behaviour prior to 1900 than the time-dependent model of Jackson (1997).

Why might our simplified time-variable flow provide a better fit to the observed ΔLOD in the 19th century than fully time-dependent tangentially geostrophic flows? The cause may be variations in the reliability of the field model from which they are derived. Throughout the 19th century, the quality, quantity and distribution of magnetic data improved considerably, in particular with a steady increase in the number of magnetic observatories. As a result, the resolution of field models also improved significantly during this period, with details of the time evolution of features becoming better resolved. This improvement is seen as a change in the nature and amount of secular variation in the field model, but is likely to be an artefact of the modelling process. Our simple temporal flow parametrization does not explain the detail of these 'features', whereas time-varying tangentially geostrophic flows allow complex variations (that may not be real) to be modelled, which could thereby contaminate the angular momentum signal in the data.

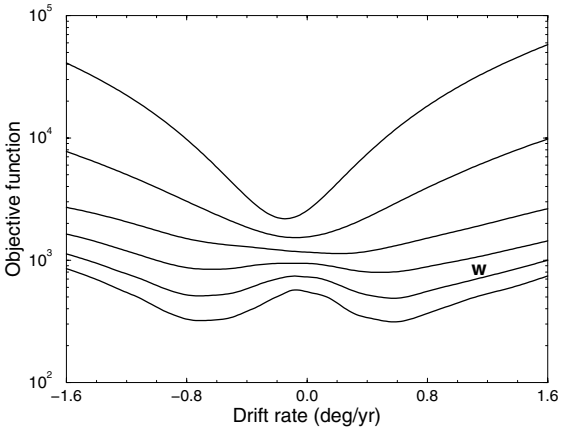

Figure 7. Objective function as a function of uniform drift rate for a variety of damping parameters for 1840–1990. For details, see caption to Fig. 1.

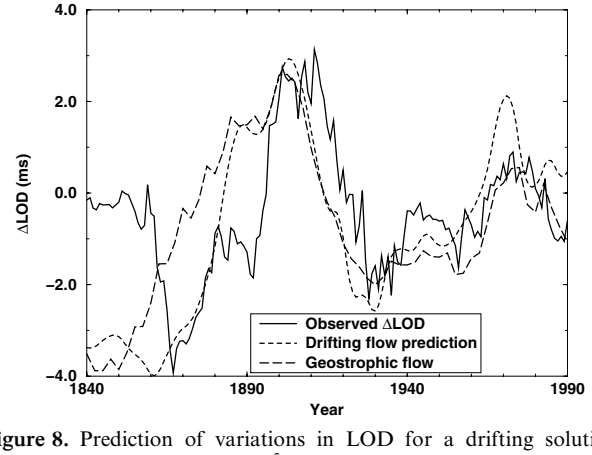

Figure 8. Prediction of variations in LOD for a drifting solution (damping parameter $\lambda_v = 2 \times 10^{-5}$) from 1840–1990, with the predictions from the tangentially geostrophic flows of Jackson *et al.* (1993) for comparison.

7 GEOPHYSICAL IMPLICATIONS

Thus far, we have considered the drifting frame as a convenient and simple mechanism to parametrize some time dependence of the flow at the cost of very few additional parameters. We now consider whether it has any physical significance beyond this computational simplicity.

A simplistic interpretation would be that on decadal timescales the drifting frame reflects the top of a rigidly rotating core, with the steady flow the surface expression of slowly varying flow driving the dynamo process. We have made this assumption to relate variations in drift rate to variations in angular momentum of the whole core. The strong surface backflow that opposes the drift could be generated by frictional coupling forces (mechanical or electromagnetic) seeking to limit the relative flow speed between the core and mantle. In this framework, the eastward-drifting solution is of particular interest. Using as a probe the axis of seismic anisotropy of the inner core, Song & Richards (1996) deduced an eastward inner core rotation rate of just over $1^\circ\ \mathrm{yr}^{-1}$ for the last 30 yr from changes in differential traveltimes, a little larger than our value of $0.8^\circ\ \mathrm{yr}^{-1}$. Subsequently, other workers (e.g. Creager 1997) also investigating body waves obtained different values. Our value falls in the middle of the range of reported results, and is thus broadly consistent with the seismic estimates if the inner and outer cores co-rotate. However, inner core rotation observations are not universally accepted (e.g. Souriau *et al.* 1997; Souriau 1998), and analysis of normal mode data implies that the inner core does not super-rotate at all (Sharrock & Woodhouse 1998; Laske & Masters 1999).

A possibly more reasonable interpretation of the drifting frame is that it represents a global wave motion, with a period of 400–500 yr, appropriate for large-scale magnetic Rossby waves or MAC waves in the core. The drifting frame then only reflects conditions at the top of the core. The idea of the secular variation being generated by wave motion is not new (Hide 1966; Gubbins & Roberts 1987). However, it has been problematic to explain the short timescale (e.g. the '60-year oscillation') of the variation. Braginsky (1984) suggested that the secular variation originates in a thin stably stratified 'hidden ocean' (Braginsky 1999) at the top of the core; the '60-year oscillation' is a manifestation of the excitation of wave modes in this layer by the torsional oscillations. Our results show that such a layer is unnecessary, and the 'oscillation' can also be explained by large-scale processes with a much longer timescale.

However, in either case, in order to explain ΔLOD, the variations in drift (the time dependence) must still reflect whole-core phenomena. In summary, we have a picture of large-scale wave motion, possibly restricted to only the top of the core, giving rise to most of the observed secular variation, with whole-core torsional oscillations superimposed. Perhaps fortuitously, our simple drifting flow parametrization is able to represent both processes.

The most unexpected result of this analysis has been the emergence of two solutions with opposite and approximately equal drift. If we interpret the drift as a wave phenomenon, this result has an attractive explanation. For simplicity, assume a uniform drift rate $\dot{\psi}$. From eq. (3), the observed velocity in the mantle frame is

$$\mathbf{u}(\theta, \phi, t) = \mathbf{u}'(\theta, \phi - \dot{\psi}t) + r_c\dot{\psi}\cos\theta\hat{\boldsymbol{\phi}}. \tag{15}$$

Now consider another flow $\mathbf{u}''$ drifting with equal and opposite angular velocity, so that

$$\mathbf{u}(\theta, \phi, t) = \mathbf{u}''(\theta, \phi + \dot{\psi}t) - r_c\dot{\psi}\cos\theta\hat{\boldsymbol{\phi}}. \tag{16}$$

Each of these flows fits the secular variation to some given tolerance. However, in the mantle frame the secular variation is linear in the flow, so that any suitably weighted linear combination of the two flows will also explain the secular variation. In particular, the average of the two flows will explain the secular variation:

$$\mathbf{u}(\theta, \phi, t) = \left[\mathbf{u}'(\theta, \phi - \dot{\psi}t) + \mathbf{u}''(\theta, \phi + \dot{\psi}t)\right]/2. \tag{17}$$

Notice that the direct contribution from the drift has been eliminated.

This allows a simple interpretation of the two solutions as two travelling waves making up a standing wave in the core, with period between 400 and 500 yr. In principal it should be possible to take the two drifting flow solutions and combine them to seek features of this standing wave. However, this is problematical, probably because the non-uniqueness of the flow inversion is obscuring this effect. The only practical way to explore this issue is to invert directly for flows of this type; this work is in progress.

8 CONCLUSIONS

A steady flow rotating by way of a drifting frame introduces some simple time dependence to the modelling of secular variation, and can significantly improve the fit to the model. Allowing this drift to be time-dependent produces little further improvement to the solution for a large increase in the number of free parameters. However, the resulting fluctuations in drift rate match those required to explain decadal variations in length of day, despite their apparently weak influence on the steady part of the flow and fit to the secular variation. Both westward and eastward drift of the core can be supported; the presence of both solutions may be indicative of a standing wave.

Further testing of the drifting flow hypothesis should soon be possible. New high-quality vector magnetic field data are becoming available from the Danish Ørsted and the German CHAMP missions. These new data will allow a correspondingly detailed analysis of recent secular variation, and hence a much more detailed comparison of the differences between time-varying geostrophic flows and our drifting flows.

Perhaps more significantly, our study suggests a new approach to the study of secular variation. Previous work can be divided into two categories: kinematic, such as this study, where a flow is constructed by modelling the observed secular variation, and dynamic, where analysis of the dynamical equations leads to suggested wave motions whose characteristics (e.g. period, general structure) are then compared with broad-scale features of the secular variation. We suggest combining these studies—using the dynamical studies to construct possible simple parametrizations of the flow structure and then fitting these parametrizations to secular variation models to determine to what extent they explain the observed signal.

ACKNOWLEDGMENTS

Much of this work was undertaken when RH was supported by a NERC postdoctoral fellowship held at the University of

Edinburgh, and KAW was Gauss Professor of the Göttingen Academy of Sciences at the Institut für Geophysik, Universität Göttingen. Further support came from NERC grant GR9/02244. We thank Dr A. Jackson for providing results from his work, and helpful reviews from Dr G. Hulot and Dr C. V. Voorhies.

REFERENCES

Backus, G.E., 1968. Kinematics of geomagnetic secular variation in a perfectly conducting core, *Phil. Trans. R. Soc. Lond.,* **A263,** 239–266.

Backus, G.E. & Le Mouël, J.-L., 1986. The region on the core-mantle boundary where a geostrophic velocity field can be determined from frozen flux magnetic data, *Geophys. J. R. astr. Soc.,* **85,** 617–628.

Bloxham, J., 1988. The dynamical regime of fluid flow at the core surface, *Geophys. Res. Lett.,* **15,** 585–588.

Bloxham, J., 1989. Simple models of fluid flow at the core surface derived from geomagnetic field models, *Geophys. J. Int.,* **99,** 173–182.

Bloxham, J., 1990. On the consequences of strong stable stratification at the top of the Earth's outer core, *Geophys. Res. Lett.,* **17,** 2081–2084.

Bloxham, J., 1992. The steady part of the secular variation of the Earth's magnetic field, *J. geophys. Res.,* **97,** 19 565–19 579.

Bloxham, J. & Jackson, A., 1991. Fluid flow near the surface of the Earth's outer core, *Rev. Geophys.,* **29,** 97–120.

Bloxham, J. & Jackson, A., 1992. Time-dependent mapping of the magnetic field at the core-mantle boundary, *J. geophys. Res.,* **97,** 19 537–19 563.

Bloxham, J., Gubbins, D. & Jackson, A., 1989. Geomagnetic secular variation, *Phil. Trans. R. Soc. Lond.,* **A329,** 415–502.

Braginsky, S.I., 1970. Torsional magnetohydrodynamic vibrations in the Earth's core and variations in day length, *Geomag. Aeronomy,* **10,** 1–8 (English translation).

Braginsky, S.I., 1984. Short-period geomagnetic secular variation, *Geophys. Astrophys. Fluid Dyn.,* **30,** 1–78.

Braginsky, S.I., 1999. Dynamics of the stably stratified ocean at the top of the core, *Phys. Earth planet. Inter.,* **111,** 21–24.

Courtillot, V., Ducruix, J. & Le Mouël, J.-L., 1978. Sur une accélération récente de la variation séculaire du champ magnétique terrestre, *C. R. Acad. Sci. Paris. Ser. D,* **287,** 1095–1098.

Creager, K., 1997. Anisotropy in the inner core from differential travel times of the phases PKP and PKIKP, *Nature,* **356,** 309–314.

Davis, R.G. & Whaler, K.A., 1996a. Determination of a steady velocity in a rotating frame of reference at the surface of the Earth's core, *Geophys. J. Int.,* **126,** 92–100.

Davis, R.G. & Whaler, K.A., 1996b. Steady flow in a drifting frame of reference at the surface of the core in the frozen-flux approximation: non-uniform drift rate, *EOS, Trans. Am. geophys. Un. Suppl.,* **77,** W144.

de Boor, C., 1978. *A Practical Guide to Splines,* Springer-Verlag, New York.

Gubbins, D., 1982. Finding core motions from magnetic observations, *Phil. Trans. R. Soc. Lond.,* **A306,** 247–254.

Gubbins, D. & Kelly, P., 1996. A difficulty with using the frozen flux hypothesis to find steady core motions, *Geophys. Res. Lett.,* **23,** 1825–1828.

Gubbins, D. & Roberts, P.H., 1987. Magnetohydrodynamics of the Earth's core, in *Geomagnetism,* Vol. 2, Chapter 1, ed. Jacobs, J.A., Academic, San Diego, CA.

Hide, R., 1966. Free hydromagnetic oscillations of the Earth's core and the theory of the geomagnetic secular variation, *Phil. Trans. R. Soc. Lond.,* **A259,** 615–650.

Hills, R.G., 1979. Convection in the Earth's mantle due to viscous shear at the core-mantle interface and due to large-scale buoyancy, *PhD thesis,* New Mexico State University, Las Cruces.

Jackson, A., 1997. Time dependency of geostrophic core surface motions, *Phys. Earth planet. Inter.,* **103,** 293–311.

Jackson, A., Bloxham, J. & Gubbins, D., 1993. Time-dependent flow at the core surface and conservation of angular momentum in the coupled core-mantle system, in *Dynamics of the Earth's Deep Interior and Earth Rotation,* pp. 97–107, eds Le Mouël, J.-L., Smylie, D.E. & Herring, T., AGU/IUGG, Washington, DC.

Jault, D. & Le Mouël, J.L., 1989. The topographic torque associated with a tangentially geostrophic motion at the core surface and inferences on flow inside the core, *Geophys. Astrophys. Fluid Dyn.,* **48,** 273–296.

Jault, D., Gire, C. & Le Mouël, J.L., 1988. Westward drift, core motions and exchanges of angular momentum between core and mantle, *Nature,* **333,** 353–356.

Laske, G. & Masters, G., 1999. Limits on differential rotation of the inner core from an analysis of the Earth's free oscillations, *Nature,* **402,** 66–69.

Le Mouël, J.-L., Gire, C. & Madden, T., 1985. Motions at the core surface in the geostrophic approximation, *Phys. Earth planet. Inter.,* **39,** 270–287.

Malin, S.R.C., Hodder, B.M. & Barraclough, D.R., 1983. Geomagnetic secular variation: a jerk in 1970, in *75th Anniversary Volume of Ebro Observatory,* pp. 239–256, ed. Cardus, J.R., Ebro Observatory, Tarragona, Spain.

McCarthy, D.D. & Babcock, A.K., 1986. The length of day since 1656, *Phys. Earth planet. Inter.,* **44,** 281–292.

Press, W.H., Flannery, B.P., Teukolsky, S.A. & Vetterling, W.T., 1986. *Numerical Recipes,* Cambridge University Press, Cambridge.

Roberts, P.H. & Scott, S., 1965. On the analysis of secular variation, 1, A hydromagnetic constraint: Theory, *J. Geomag. Geoelectr.,* **17,** 137–151.

Sharrock, D.S. & Woodhouse, J.H., 1998. Investigation of time dependent inner core structure by the analysis of free oscillation spectra, *Earth Planets Space,* **50,** 1013–1018.

Song, X.D. & Richards, P.G., 1996. Seismological evidence for differential rotation of the Earth's inner core, *Nature,* **382,** 221–224.

Souriau, A., 1998. New seismological constraints on differential rotation of the inner core from Novaya Zemlya events recorded at DRV, Antarctica, *Geophys. J. Int.,* **134,** F1–F5.

Souriau, A., Roudil, P. & Moynot, B., 1997. Inner core differential rotation: facts and artefacts, *Geophys. Res. Lett.,* **24,** 2103–2106.

Voorhies, C.V., 1986. Steady surficial core motions: an alternate method, *Geophys. Res. Lett.,* **13,** 1537–1540.

Voorhies, C.V. & Backus, G.E., 1985. Steady flows at the top of the core from geomagnetic-field models—the steady motions theorem, *Geophys. Astrophys. Fluid Dyn.,* **32,** 163–173.

Wessel, P. & Smith, W.H.F., 1991. Free software helps map and display data, *EOS, Trans. Am. geophys. Un.,* **72,** 445–446.

Whaler, K.A., 1980. Does the whole of the Earth's core convect?, *Nature,* **287,** 528–530.

Whaler, K.A., 1986. Geomagnetic evidence for fluid upwelling at the core-mantle boundary, *Geophys. J. R. astr. Soc.,* **86,** 563–588.

Whaler, K.A. & Davis, R.G., 1997. Probing the Earth's core with geomagnetism, in *Earth's Deep Interior,* pp. 114–166, ed. Crossley, D.J., Gordon & Breach, Amsterdam.